Effects of Individualized Gait Rehabilitation Robotics for Gait Training on Hemiplegic Patients: Before-After Study in the Same Person

Zhao Guo [1†], Jing Ye [2†], Shisheng Zhang [3], Lanshuai Xu [2], Gong Chen [2], Xiao Guan [4], Yongqiang Li [5*] and Zhimian Zhang [4,6*]

[1] School of Power and Mechanical Engineering, Wuhan University, Wuhan, China, [2] Shenzhen Milebot Robotics Co., Ltd., Shenzhen, China, [3] School of Mechanical Engineering, Shenyang Jianzhu University, Shenyang, China, [4] Department of Health Management Center, Qilu Hospital, Shandong, China, [5] Rehabilitation Medicine Center, The First Affiliated Hospital, Nanjing Medical University, Nanjing, China, [6] The Cheeloo College of Medicine, Shandong University, Jinan, China

Background: Lower-limb exoskeleton robots are being widely used in gait rehabilitation training for patients with stroke. However, most of the current rehabilitation robots are guided by predestined gait trajectories, which are often different from the actual gait trajectories of specific patients. One solution is to train patients using individualized gait trajectories generated from the physical parameters of patients. Hence, we aimed to explore the effect of individual gaits on energy consumption situations during gait rehabilitation training for hemiplegic patients with lower-limb exoskeleton robots.

Methods: A total of 9 unilateral-hemiplegic patients were recruited for a 2-day experiment. On the first day of the experiment, the 9 patients were guided by a lower-limb exoskeleton robot, walking on flat ground for 15 min in general gait trajectory, which was gained by clinical gait analysis (CGA) method. On the other day, the same 9 patients wore the identical robot and walked on the same flat ground for 15 min in an individualized gait trajectory. The main physiological parameters including heart rate (HR) and peripheral capillary oxygen saturation (SpO2) were acquired *via* cardio tachometer and oximeter before and after the walking training. The energy consumption situation was indicated by the variation of the value of HR and SpO2 after walking training compared to before.

Results: Between-group comparison showed that the individualized gait trajectory training resulted in an increase in HR levels and a decrease in SpO2 levels compared to the general gait trajectory training. The resulting difference had a statistical significance of $p < 0.05$.

Conclusion: Using individualized gait guidance in rehabilitation walking training can significantly improve energy efficiency for hemiplegic patients with stroke.

Keywords: individualized gait, hemiplegic patient, gait rehabilitation, exoskeleton robot, stroke

INTRODUCTION

Globally, stroke, which is a major cause of limb functional disabilities, is the disease with the highest disability rate (80 ∼ 90%). In recent years, the population of patients with stroke continues to grow at a rate of nearly 9% every year (Liu et al., 2007), and it shows a trend in the youth community. The disease is causing permanent serious harm to the patients and brings a heavy medical burden to patients' families and society.

In recent years, more and more attention has been paid to the application of exoskeleton robots in the field of rehabilitation, in particular neurorehabilitation. The rehabilitation robot, such as LOPES (Meuleman et al., 2015), Lokomat (Riener et al., 2010), WalkTrainer (Stauffer et al., 2008), ALEX (Banala et al., 2008), Indego (Hartigan et al., 2015), HAL (Tsukahara et al., 2014), ReWalk (Esquenazi et al., 2012), Ekso (Kozlowski et al., 2015), replace the rehabilitation physician to provide physical therapy to patients and to carry out safe and reliable repetitive training for patients, which help to reduce the workload of rehabilitation physician in physical therapy and improve the effectiveness of rehabilitation treatment (Meng et al., 2015).

In the above devices, a gait control strategy based on finite state or predetermined gait trajectory is adopted. These general gait trajectories of hip joint, knee joint, and ankle joint are the statistical results of many healthy people (J Robert Close, 1952; Murray et al., 1964; Johnston and Smidt, 1969). However, many studies have shown that physical factors—walking speed, gender, age, and other anthropometric parameters—led to different gait patterns in different groups (Wang et al., 2003; Kale et al., 2004). The existing wearable exoskeleton control strategy cannot meet individual differences for different users (Chen et al., 2016). In order to provide specific gait guidance for exoskeleton wearers, gait prediction has become a popular research branch (Zhang and Ma, 2019; Khera and Kumar, 2020). Vallery et al. (2008) proposed a complementary limb motion estimation algorithm, which can generate real-time trajectory to provide compensation for hemiplegic patients, but its goal is to achieve the symmetry between legs, rather than periodic gait sequence. Kagawa et al. (2015) proposed the method of motion planning control in joint space to provide variable step length and speed for exoskeleton, but the gait mode is not natural, because the limited fixed joint angle is predefined for trajectory planning. However, these studies lack clinical verification. Rajasekaran et al. (2018) applied a brain-computer interface to exoskeleton control and conducted clinical trials on 4 patients with spinal cord injury. However, when there is no auxiliary trajectory guidance, it is difficult for patients to walk normally after rehabilitation.

Our study aimed to examine the energy consumption effects of individualized gait trajectory in walking rehabilitation among nine patients with hemiplegic status-post stroke with the assistance of a lower-limb exoskeleton robot named BEAR-H1. This paper proposed a clinical metric for measuring a patient's energy consumption level after walking rehabilitation. Heart rate (HR) and peripheral capillary oxygen saturation (SpO2) are selected as the independent variables to reflect the energy level of walking guided by an individualized gait trajectory compared with that of walking guided by a general gait trajectory, which is a locomotion data from Clinical Gait Analysis (CGA).

We combined Fast Fourier Transformation (FFT) and Gaussian Process Regression (GPR) to generate individualized gait trajectories, which could be adjusted according to different patients. The proposed individualized gait trajectory generation algorithm was tested with the cross-validation method. The high accuracy and strong robustness of the algorithm were validated referring to the CGA data. The Mean Absolute Error (MAE) and the SD of predicted joint rotation angles of the individualized gait trajectories were optimized to the most extent. Finally, the algorithm was applied to a new lower extremity exoskeleton BEAR-H1 to train patients (Yun et al., 2014; Kong et al., 2018). Nine stroke patients with different morphological parameters were recruited for a clinical trial, which was helpful to observe the diversified behaviors of rehabilitation strategies.

Training results showed that compared to general gait trajectory, there was an increase in HR and a decrease in SpO2 when the robot was controlled by individualized gait trajectories. Specifically, changes in HR were more significant. On the contrary, changes in SpO2 were much smaller. This contrast indicated that the individualized gait strategy was energy friendly for hemiplegic patients.

EXOSKELETON BEAR-H1 PLATFORM

BEAR-H1 is a wearable, battery-powered lower-limb rehabilitation robot with initiative assisting technology, and it enables gait events to be detected when the subjects are wearing the BEAR-H1, as shown in **Figure 1** left panel. The robot, which has three active degrees of freedom and a passive degree of freedom on each leg, is self-developed to help patients with hemiplegia conduct rehabilitation training. The three degrees of freedom are rotations along the hip joint, the knee joint, and the ankle joint on the sagittal plane and they are actuated by motors (Santos et al., 2012). The adduction and abduction of the hip joint is the passive degree of freedom (Kotwicki et al., 2008). There is a rotary encoder in each joint of BEAR-H1, as shown in **Figure 1** left panel, which is used to measure the real-time angle of each joint (Zhang et al., 2015). The actuator can accurately control the joint angle by the feedback of the encoder. The gait trajectories, as shown in **Figure 1** right panel, can be changed easily by modifying the program of the robot.

For the purpose of the present study, we embedded different individualized gait trajectories that was corresponding to specific patient's training into the internal storage in the micro-controller unit in advance. The control process was executed at 1,000 Hz and the testing time for the patient wearing the BEAR-H1 was about 15 min. The level of assistance was variable according to the patient's actual walking ability level.

INDIVIDUALIZED GAIT RECONSTRUCTION

The generation process for individualized gait reconstruction includes four components. As shown in **Figure 2**, the input
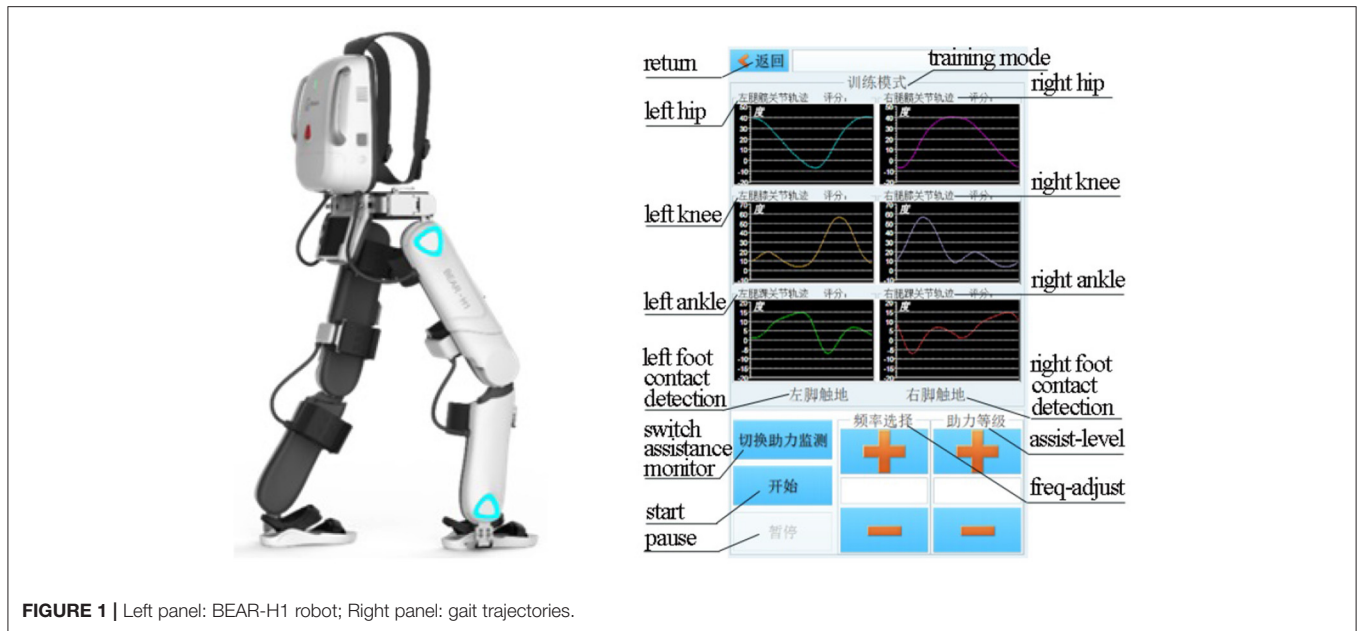
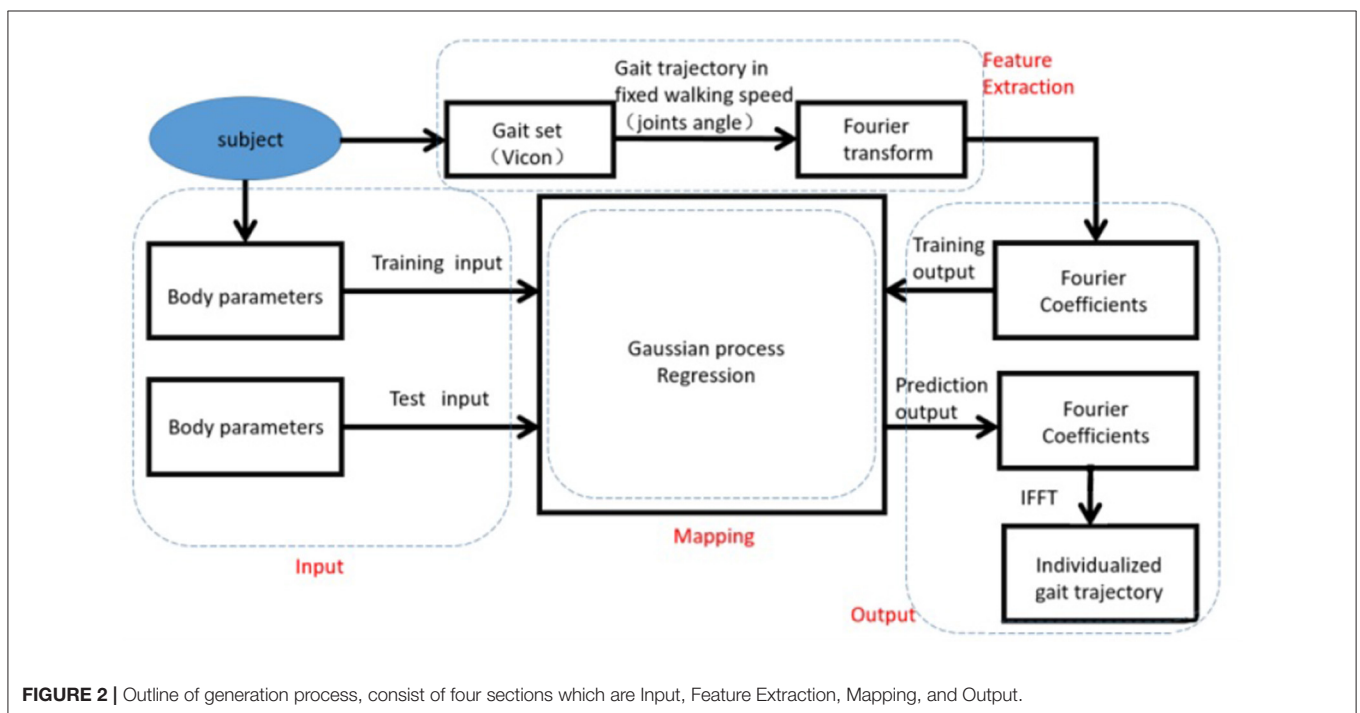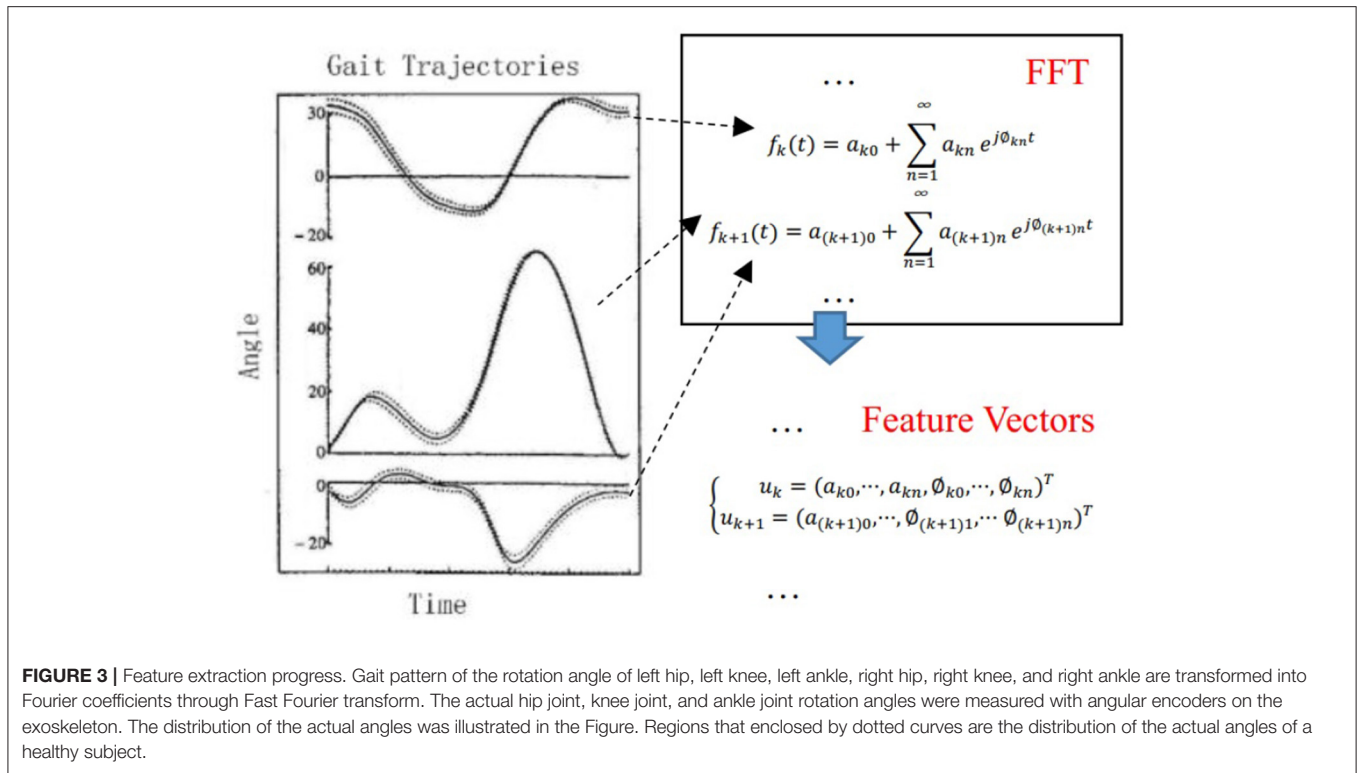FIGURE 1 | Left panel: BEAR-H1 robot; Right panel: gait trajectories.

FIGURE 2 | Outline of generation process, consist of four sections which are Input, Feature Extraction, Mapping, and Output.

component is consisted of body parameters only. Gait data is divided into various sets according to different waking speeds. A certain walking speed is selected, linking to a specific set for feature extraction. During the feature extraction, encoding progress employs an explicable model for apprehensible processing which is Fourier Transform. Correspondingly, decoding and reconstruction for generating the final individualized gait pattern are finished by Fourier Inversion at the output component.

In order to establish the mapping relationships between the body parameters and the gait pattern, the gait pattern is first extracted into Fourier Coefficients to reduce the computational cost from numerous data points to handful coefficients (Reddy and Rani, 2016). The Fourier Coefficients can be predicted through GPR with body parameters. Finally, the individualized gait pattern is reconstructed based on predictive Fourier Coefficients.

FIGURE 3 | Feature extraction progress. Gait pattern of the rotation angle of left hip, left knee, left ankle, right hip, right knee, and right ankle are transformed into Fourier coefficients through Fast Fourier transform. The actual hip joint, knee joint, and ankle joint rotation angles were measured with angular encoders on the exoskeleton. The distribution of the actual angles was illustrated in the Figure. Regions that enclosed by dotted curves are the distribution of the actual angles of a healthy subject.

Gait Feature Extraction and Anthropometry

Gait patterns are represented as the trajectories of lower-limb joints, which are joints of hips, knees, and ankles (Isola et al., 2011). Although gait patterns determined various gait features, they are time-sequence signals with the periodic pattern (Trivino et al., 2010), which is the most often domain applied with Fourier Transform (Morgan and Noehren, 2018).

Fourier transform is a traditional spectral analysis method to describe any periodic signal in its harmonic components (Winter, 2009). Since walking is periodic and the power for walking is supplied rhythmically with temporal consistency (Winter, 2009), Fourier transform is often used to describe the frequency content of gait (Antonsson and Mann, 1985; Chau, 2001). In our study, each joint angle waveform was analyzed in the frequency domain and decomposed into one Fourier coefficient and frequency vector as the gait features:

$$\mu_k = (a_{k0}, \cdots, a_{kn}, \phi_{k1}, \cdots, \phi_{kn})^T \tag{1}$$

where a_{kn} is the Fourier coefficients, $\phi_k n$ is the frequency of harmonic wave, and k is the number of walking trials. Note that $\phi_0 = 0$. In this paper, we take $n = 3$. Feature extraction progress is shown in **Figure 3**.

Gait patterns are determined by various factors. To fully study the influence of different parameters on the gait pattern, a total of 28 body parameters are considered in this paper, as shown in **Figure 4**. Then, the vector of body parameters for the ith human subject can be formulated as.

$$B_i = (b_1, \cdots, b_{28})^T \tag{2}$$

Gaussian Process Regression

In order to obtain the mapping relationship between each gait feature u and human body parameters B. We implemented the GPR algorithm for achieving our goal since gait feature prediction is regarded as a nonlinear regression task. As a kernel-based statistical learning method, GPR is with advantages for solving the small sample learning problem (Cen et al., 2021), which suits the scenario that limited human subjects are included in the database. A detailed description of GPR can be studied in Rasmussen and Williams (2006).

The performance of the proposed scheme can be assessed by comparing the difference between the generated gait and the actual gait of the subject (i.e., measured by the sensor), in terms of the correlation coefficient (3) and the mean absolute error (MAE) (4). A higher correlation coefficient between the predicted and actual and smaller values of MAE implies a better performance of the proposed scheme, and vice versa (Mukaka, 2012; Mundt et al., 2020).

$$\rho = \frac{cov\left(\tilde{\theta}, \hat{\theta}\right)}{\sqrt{var\left(\tilde{\theta}\right) var\left(\hat{\theta}\right)}} \tag{3}$$

$$e_{MAE} = \sum_{i=1}^{L_0} \frac{\left|\hat{\theta}_i - \tilde{\theta}_i\right|}{L_0} \tag{4}$$
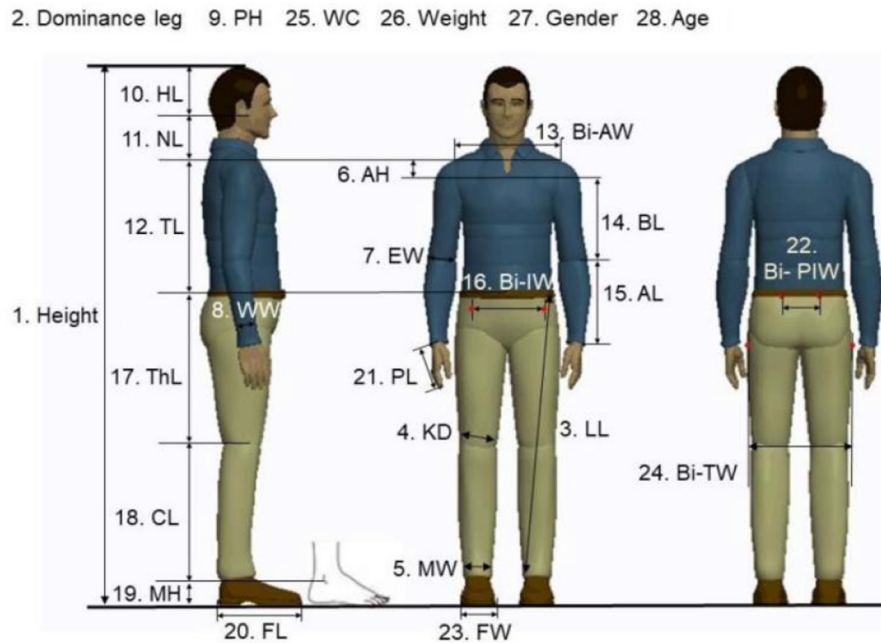
FIGURE 4 | Gait related body parameters 3. LL: Leg Length; 4. KD: knee diameter; 5. MW: Malleolus width; 6. AH: Acromion height; 7. EW: Elbow width; 8. WW: Wrist width; 9. PH: Palm height; 10. HL: Head length; 11. NL: Neck length; 12. TL: Trunk length; 13. Bi-AW: Bi-acromion width; 14. BL: Brachium length;15. AL: Antebrachium length; 16. Bi-IW: Bi-iliac width; 17. ThL: Thigh length; 18. CL: Calf length; 19. MH: Malleolus height; 20. FL: Foot Length; 21. PL: Palm length; 22. Bi-PIW: Bi-posterior iliac; 23. FW: Foot width; 24. Bi-TW: Bi-trochanteric width; 25. WC: Waist circumference.

TABLE 1 | Mean absolute errors (MAEs) of subjects results from Clinical Gait Analysis (CGA) for comparison.

Joints	GPR(deg)	CGA(deg)
Hip(L)	3.36(1.03)	7.66(1.78)
Knee(L)	4.21(1.64)	9.28(3.07)
Ankle(L)	3.35(1.42)	
Hip(R)	3.47(1.18)	7.66(1.78)
Knee(R)	4.51(1.11)	9.28(3.07)
Ankle(R)	3.40(1.25)	

L: left side; R: right side.

TABLE 2 | Correlation coefficients of subjects and results from CGA for comparison.

Joints	GPR(deg)	CGA(deg)
Hip(L)	0.99(0.01)	0.87(0.07)
Knee(L)	0.97(0.02)	0.85(0.11)
Ankle(L)	0.92(0.04)	
Hip(R)	0.98(0.01)	0.87(0.07)
Knee(R)	0.95(0.02)	0.85(0.11)
Ankle(R)	0.94(0.04)	

L: left side; R: right side.

Where L_0 is the fixed length to which the gait cycle is resampled to. $\tilde{\theta}_i$ is the ith actual angle of joint after resampling. $\hat{\theta}_i$ is the ith predicted angle of joint.

Algorithm Performance

The performance of the proposed algorithm was validated by the cross-validation method using the training set. Due to the limited data and to make full use of it, a leave-one-out method was chosen to validate this algorithm's robustness (Tsumoto and Hirano, 2014; Wong, 2015). The formula (4) defines the MAE to measure the degree of deviation of the predicted gait trajectory from the real trajectory. The average MAEs of each joint for all subjects and CGA results are presented in **Table 1** for the leave-one-out method. For comparison, the mean and SD for each joint

are also given, as well as the mean and SDs obtained by the CGA (Cen et al., 2021) methods. The means and SDs of MAEs obtained by GPR are both smaller than those obtained by the CGA (no data of ankle are provided by CGA). This also suggests that the trajectory predicted by GPR is closer to the real trajectory, and the MAEs of different subjects have fewer fluctuations. In **Table 2**, the means (SDs) of correlation coefficients of each joint for five subjects at different as well as the results from CGA are shown. By comparison, the correlation coefficients obtained by GPR are also better than those obtained by CGA. Therefore, according to the correlation analysis, the IGPG method gives a better prediction with a strong correlation.

Clinical Gait Analysis is a process of evaluating the locomotion patterns of patients with specific gait-related

TABLE 3 | Participants' demographics (N = 9).

Subject	Age	Gender	Height (cm)	Weight (kg)	Paretic side	FAC	Diagnosis
1	42	Male	174	77	Left	IV	The cerebral thrombosis
2	40	Male	170	63	Left	IV	The putamen hemorrhage
3	47	Male	160	58	Right	III	The putamen hemorrhage
4	56	Female	153	51	Right	IV	The putamen hemorrhage
5	65	Male	169	90	Left	III	The cerebral thrombosis
6	40	Male	166	72	Left	IV	The cerebral thrombosis
7	33	Male	165	85	Right	III	The putamen hemorrhage
8	69	Male	165	70	Right	III	The putamen hemorrhage
9	42	Male	168	75	Left	IV	The cerebral thrombosis

abnormalities. It is an open-source platform to the public and its data has been uploaded from institutes all over the world. Gait analysis may be executed in a gait analysis laboratory using specialized instruments, such as Vicon Motion Capturing System. This is also referred to as computerized gait analysis, quantitative gait analysis, or CGA. This procedure has been used to understand the etiology of gait abnormalities.

SUBJECTS AND METHODS

Experiment Criteria

The participants were nine patients (eight men and one woman with mean age=48.22 years) with hemiplegia status-post stroke, who resided in a convalescent rehabilitation ward. All participants had their stroke within 12 months and they had residual right hemiplegia. The demographics of participants are presented in **Table 3**.

Inclusion criteria were as follows:

- First stroke with hemiplegia.
- Functional ambulation category (FAC) of III or IV for the leg.
- Independent or supervision-only walking ability with a quad cane or T cane or no support tool.
- Participants provided written informed consent after the purpose of the study was explained.

Participants were excluded based on the following criteria:

- Unable to understand study-related procedures.
- Exhibited serious hypertension on walking.
- With circulatory disease, respiratory disease, or extreme weakness.
- Failed to receive physical clearance to participate.

Experiment Protocol

The experiment was conducted for a total of 2 days.

On the first day of the experiment, 9 patients wore the exoskeleton robot, guided by general gait trajectory which reflects the motion of hip, knee, and ankle joint on healthy people (Murray et al., 1964; Johnston and Smidt, 1969), and received walking training (**Figure 5**) for 15 min at a fixed frequency.

FIGURE 5 | Exoskeleton-robot-assisted walking training.
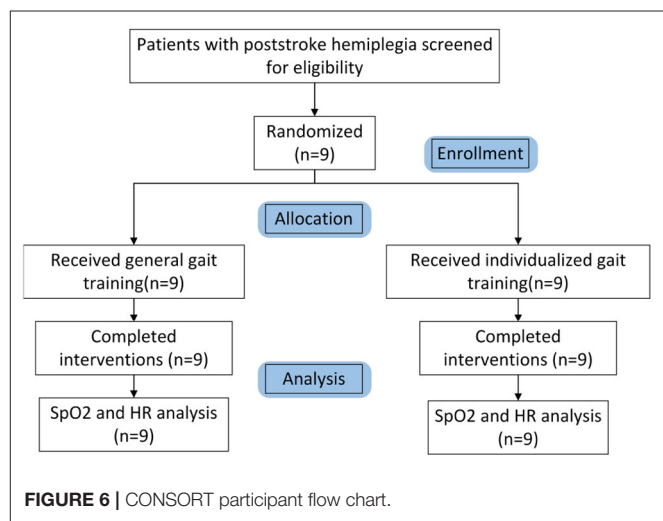
FIGURE 6 | CONSORT participant flow chart.

On the second day of the experiment, the individualized gait which was generalized by our method was applied to the exoskeleton robot to train the same 9 patients with the same method.

Dependent variables are HR and SpO2. Dependent variables were sampled four times for each patient: before and after the last individualized-gait exercise treatment, before and after the last general-gait exercise treatment. The effectiveness of the algorithm was verified by comparing patients' decrease of SpO2 and the increase of HR when they were guided by individualized gait trajectory and general gait trajectory, respectively (**Figure 6**).

The purpose of the experiment is explained to each patient and written informed consents are required to be signed by patients.

RESULT

Experiments were administered over 2 days totally, during which the patients were trained by general gait trajectory and individualized gait trajectory sequentially. Results are presented in **Tables 4**, **5**.

TABLE 4 | Results of general-gait-guided treatment.

	Evaluation items	Prior to treatment	After treatment	variation
Subject 1	SpO2 (%)	96	91	-5
	HR(bpm)	80	88	8
Subject 2	SpO2 (%)	97	96	−1
	HR(bpm)	82	104	22
Subject 3	SpO2 (%)	98	96	−2
	HR(bpm)	105	120	15
Subject 4	SpO2 (%)	97	96	−1
	HR(bpm)	96	109	13
Subject 5	SpO2 (%)	97	95	-2
	HR(bpm)	82	89	7
Subject 6	SpO2 (%)	98	97	−1
	HR(bpm)	77	89	12
Subject 7	SpO2 (%)	99	96	-3
	HR(bpm)	82	91	9
Subject 8	SpO2 (%)	98	94	−4
	HR(bpm)	76	89	13
Subject 9	SpO2 (%)	98	96	−2
	HR(bpm)	81	79	−2

TABLE 5 | Result of individualized-gait-guided treatment.

	Evaluation items	Prior to treatment	After treatment	variation
Subject 1	SpO2 (%)	97	95	–2
	HR(bpm)	80	74	–6
Subject 2	SpO2 (%)	96	96	0
	HR(bpm)	90	105	15
Subject 3	SpO2 (%)	97	96	–1
	HR(bpm)	107	113	6
Subject 4	SpO2 (%)	97	98	1
	HR(bpm)	103	113	10
Subject 5	SpO2 (%)	98	97	–1
	HR(bpm)	83	87	4
Subject 6	SpO2 (%)	98	97	–1
	HR(bpm)	75	84	9
Subject 7	SpO2 (%)	99	98	–1
	HR(bpm)	80	88	8
Subject 8	SpO2 (%)	98	96	–2
	HR(bpm)	79	83	4
Subject 9	SpO2 (%)	98	98	0
	HR(bpm)	78	79	1

- Changes after walking training with exoskeleton robot—we observed changes in SpO2 (**Figure 7**) and HR (**Figure 8**) between the before treatment and after treatment in 2 days, respectively. Specifically, changes in HR were more significant. On the contrary, changes in SpO2 were much smaller.

- Differences between two rehabilitation training—from the data collected in the two training sessions, we observed similar varying trends in SpO2 and HR between the before treatment and after treatment. In both groups, the levels of SpO2 decreased and the levels of HR increased (except in rare cases, the levels of HR decreased and the level of SpO2 increased or both remained unchanged. Overall, there was a significant difference in the degree of changes in the levels of SpO2 and HR between two rehabilitation training.) Patients had a smaller SpO2 reduction and larger HR increment when they were guided by the individualized gait trajectory.

- Differences between patients—in both training sessions, the SpO2 levels of different patients before receiving the treatment were roughly the same but started to have slight differences after patients received the individualized treatment, while the HR levels of different patients before and after receiving the treatment was very different. Besides, the degree of dispersion of changes in patients' HR and SpO2 levels under the guidance of two gait trajectories was different. When patients were assisted by the individualized gait trajectories, they had a smaller SD of the changed values of HR and SpO2 levels.

DISCUSSION AND CONCLUSIONS

Lower extremity robotic exoskeleton devices perform the repetitive practice of specific functional tasks in rehabilitation therapy, such as walking training. For each hemiplegic patient, we generalize individualized gaits for their specific training.

This study is to examine the energy consumption effects of individualized gait in walking training among nine patients with hemiplegia status-post stroke with the assistance of a lower-limb exoskeleton robot. HR and peripheral capillary oxygen saturation (SpO2) are selected as the independent variables to reflect energy consumption level (Christensen et al., 1983; Hiilloskorpi et al., 2003). **Tables 4**, **5** show that SpO2 decreases and HR increases during the walking training. It reveals that our measurement result is acceptable because the internal oxygen is consumed and the heartbeats have a higher frequency to provide blood where the oxygen is stored during the training process. For all patients, the levels of SpO2 are similar but the values of HR are various, showing that the physiological conditions are different among patients. Different HRs are needed to maintain a required blood oxygen level to support their physiological activity. In **Table 5**, compared to **Table 4**, the decrease of SpO2 is generally smaller and the HR is also with a tinier change. **Tables 6**, **7** express the same view precisely. From the aspect of SpO2, the decrease is 2.33% in general-gait-treatment which is larger than the SpO2 level in individualized-gait treatment - 0.78% in average. The HR increases by 10.78 beats per min in general-gait treatment, whereas it is 5.67 beats-per-min growth in individualized-gait treatment. SpO2 and HR are related to the extent of effort the patients made during the walking training period (Fan et al., 2017; Mohan et al., 2017; Nemcova et al., 2020). The more effort they made while walking, the larger proportion of SpO2 decrease and HR increase. As human gaits have specific pattern for each individual, walking with a general gait means the mismatching to original walking habits and therefore patients have to make more effort to
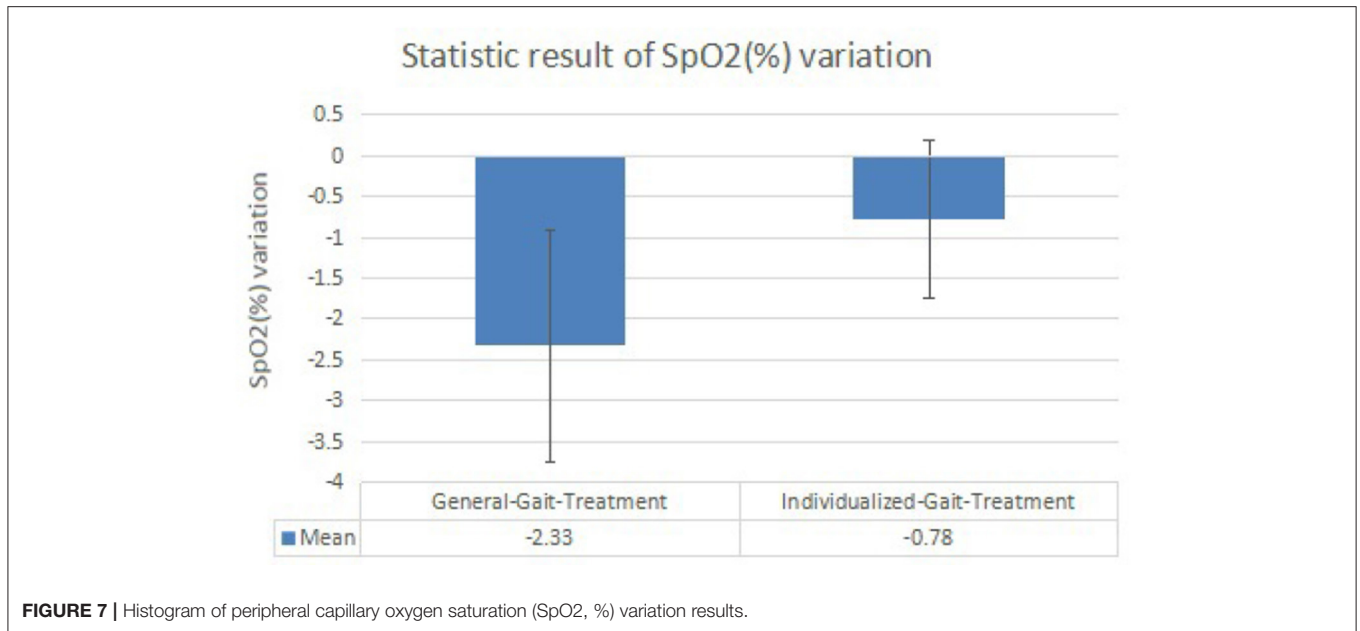
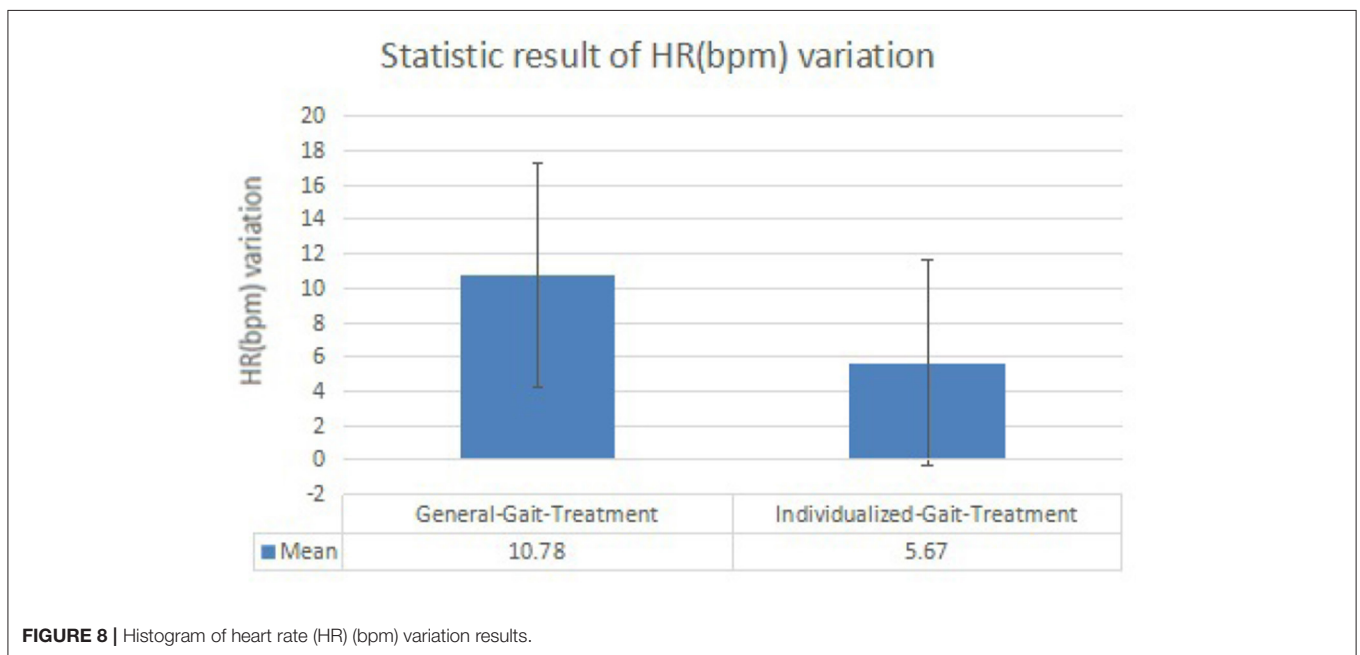**FIGURE 7 |** Histogram of peripheral capillary oxygen saturation (SpO2, %) variation results.

FIGURE 8 | Histogram of heart rate (HR) (bpm) variation results.

TABLE 6 | Statistic result of peripheral capillary oxygen saturation (SpO2) (%) variation.

	Subject 1	Subject 2	Subject 3	Subject 4	Subject 5	Subject 6
General-gait-treatment	−5	−1	−2	−1	−2	-1
Individualized-gait treatment	−2	0	−1	1	−1	−1

	Subject 7	Subject 8	Subject 9	Mean	STD	
General-gait-treatment	−3	−4	−2	−2.33	1.1414	
Individualized-gait treatment	−1	−2	0	−0.78	0.972	

TABLE 7 | Statistic result of heart rate (HR) (%) variation.

	Subject 1	Subject 2	Subject 3	Subject 4	Subject 5	Subject 6
General-gait-treatment	8	22	15	13	7	12
Individualized-gait treatment	-6	15	6	10	4	9

	Subject 7	Subject 8	Subject 9	Mean	STD
General-gait-treatment	9	13	−2	10.78	6.553
Individualized-gait treatment	8	4	1	5.67	5.979

overcome the inconformity to follow the gait pattern of the exoskeleton robot. On the other hand, the individualized gait reduces the inconformity between patients and the exoskeleton robot, therefore patients can follow the robot's guidance easier during walking rehabilitation training. Thus, the individualized gait saves energy consumption, and, therefore, the training time for hemiplegic patients can be expanded since more energy remains.

In the future, more metabolic parameters, i.e., the CO_2 and O_2 content in exhaled gas, more patients, and more novel algorithms for gait generalizing will be investigated to find out the different energy consumption situation. A formal clinical will be conducted to verify that the individualized-gait exoskeleton robot has positive effects on rehabilitation for hemiplegic patients.

DATA AVAILABILITY STATEMENT

The original contributions presented in the study are included in the article/supplementary material, further inquiries can be directed to the corresponding authors.

ETHICS STATEMENT

The studies involving human participants were reviewed and approved by Research Ethics Committee of Qilu Hospital of Shandong University. The patients/participants provided their written informed consent to participate in this study.

AUTHOR CONTRIBUTIONS

JY, ZG, and GC made substantial contributions to experimental design. SZ and LX are in charge of data collection, data analysis, and drafting the manuscript. YL, ZZ, and XG offered their expertise advice in screening the subjects, supervising the clinical trial, and interpreting the results. All authors have read and approved the final manuscript.

FUNDING

ACKNOWLEDGMENTS

REFERENCES

Antonsson, E. K., and Mann, R. W. (1985). The frequency content of gait. *J. Biomech.* 18, 39–47. doi: 10.1016/0021-9290(85)90043-0

Banala, S. K., Kim, S. H., Agrawal, S. K., and Scholz, J. P. (2008). Robot assisted gait training with active leg exoskeleton (alex). *IEEE Trans. Neural Syst. Rehabil. Eng.* 17, 2–8. doi: 10.1109/BIOROB.2008.4762885

Cen, R., Jiang, T., and Tang, P. (2021). Modified gaussian process regression based adaptive control for quadrotors. *Aerospace Sci. Technol.* 110:106483. doi: 10.1016/j.ast.2020.106483

Chau, T. (2001). A review of analytical techniques for gait data. part 2: neural network and wavelet methods. *Gait Posture*, 13, 102–120. doi: 10.1016/S0966-6362(00)00095-3

Chen, B., Ma, H., Qin, L.-Y., Gao, F., Chan, K.-M., Law, S.-W., et al. (2016). Recent developments and challenges of lower extremity exoskeletons. *J. Orthopaedic Transl.* 5, 26–37. doi: 10.1016/j.jot.2015.09.007

Christensen, C. C., Frey, H. M., Foenstelien, E., Aadland, E., and Refsum, H. E. (1983). A critical evaluation of energy expenditure estimates based on individual O_2 consumption/heart rate curves and average daily heart rate. *Am. J. Clin. Nutr.* 37, 468–472. doi: 10.1093/ajcn/37.3.468

Esquenazi, A., Talaty, M., Packel, A., and Saulino, M. (2012). The rewalk powered exoskeleton to restore ambulatory function to individuals with thoracic-level motor-complete spinal cord injury. *Am. J. Phys. Med. Rehabil.* 91, 911–921. doi: 10.1097/PHM.0b013e318269d9a3

Fan, F., Yan, Y., Tang, Y., and Zhang, H. (2017). A motion-tolerant approach for monitoring spo2 and heart rate using photoplethysmography signal with dual frame length processing and multi-classifier fusion. *Comput. Biol. Med.* 91, 291–305. doi: 10.1016/j.compbiomed.2017.10.017

Hartigan, C., Kandilakis, C., Dalley, S., Clausen, M., Wilson, E., Morrison, S., et al. (2015). Mobility outcomes following five training sessions with a powered exoskeleton. *Top. Spinal Cord. Inj. Rehabil.* 21, 93–99. doi: 10.1310/sci2102-93

Hiilloskorpi, H., Pasanen, M., Fogelholm, M., Laukkanen, R. M., and Mänttäri, A. (2003). Use of heart rate to predict energy expenditure from low to high activity levels. *Int. J. Sports Med.* 24, 332–336. doi: 10.1055/s-2003-40701

Isola, P., Xiao, J., Torralba, A., and Oliva, A. (2011). What makes an image memorable? In CVPR 2011, pages 145-152. IEEE. doi: 10.1109/C.V.P.R.2011.5995721

J Robert Close, V. T. I. (1952). *The Action of the Ankle Joint*. Berkeley, CA: University of California.

Johnston, R. C., and Smidt, G. L. (1969). Measurement of hip-joint motion during walking: evaluation of an electrogoniometric method. *J. Bone Joint. Surg. Am.* 51, 1083–1094. doi: 10.2106/00004623-196951060-00003

Kagawa, T., Ishikawa, H., Kato, T., Sung, C., and Uno, Y. (2015). Optimization-based motion planning in joint space for walking assistance with wearable robot. *IEEE Trans. Rob.* 31, 415–424. doi: 10.1109/TRO.2015.2409434

Kale, A., Sundaresan, A., Rajagopalan, A., Cuntoor, N. P., Roy-Chowdhury, A. K., Kruger, V., et al. (2004). Identification of humans using gait. *IEEE Trans. Image Process.* 13, 1163–1173. doi: 10.1109/TIP.2004.832865

Khera, P., and Kumar, N. (2020). Role of machine learning in gait analysis: a review. *J. Med. Eng. Technol.* 44, 441–467. doi: 10.1080/03091902.2020.1822940

Kong, D., Chen, Y., and Li, N. (2018). Gaussian process regression for tool wear prediction. *Mech. Syst. Signal Process.* 104, 556–574. doi: 10.1016/j.ymssp.2017.11.021

Kotwicki, T., Walczak, A., and Szulc, A. (2008). Trunk rotation and hip joint range of rotation in adolescent girls with idiopathic scoliosis: does the" dinner plate" turn asymmetrically? *Scoliosis* 3, 1–11. doi: 10.1186/1748-7161-3-1

Kozlowski, A., Bryce, T., and Dijkers, M. (2015). Time and effort required by persons with spinal cord injury to learn to use a powered exoskeleton for assisted walking. *Top. Spinal Cord. Inj. Rehabil.* 21, 110–121. doi: 10.1310/sci2102-110

Liu, M., Wu, B., Wang, W.-Z., Lee, L.-M., Zhang, S.-H., and Kong, L.-Z. (2007). Stroke in china: epidemiology, prevention, and management strategies. *Lancet Neurol.* 6, 456–464. doi: 10.1016/S1474-4422(07)70004-2

Meng, W., Liu, Q., Zhou, Z., Ai, Q., Sheng, B., and Xie, S. S. (2015). Recent development of mechanisms and control strategies for robot-assisted lower limb rehabilitation. *Mechatronics* 31, 132–145. doi: 10.1016/j.mechatronics.2015.04.005

Meuleman, J., Van Asseldonk, E., Van Oort, G., Rietman, H., and Van Der Kooij, H. (2015). Lopes ii–design and evaluation of an admittance controlled gait training robot with shadow-leg approach. *IEEE Trans. Neural Syst. Rehabil. Eng.* 24, 352–363. doi: 10.1109/TNSRE.2015.2511448

Mohan, P. M., Nagarajan, V., and Nisha, A. A. (2017). "A frame work to estimate heart rate and arterial oxygen saturation (spo2)," in *2017 International Conference on Communication and Signal Processing (ICCSP)* (Chennai: IEEE), 1645–1648.

Morgan, K. D., and Noehren, B. (2018). Identification of knee gait waveform pattern alterations in individuals with patellofemoral pain using fast fourier transform. *PLoS ONE* 13:e0209015. doi: 10.1371/journal.pone.0209015

Mukana, M. M. (2012). A guide to appropriate use of correlation coefficient in medical research. *Malawi Med. J.* 24, 69–71.

Mundt, M., Thomsen, W., Witter, T., Koeppe, A., David, S., Bamer, F., et al. (2020). Prediction of lower limb joint angles and moments during gait using artificial neural networks. *Med. Biol. Eng. Comput.* 58, 211–225. doi: 10.1007/s11517-019-02061-3

Murray, M. P., Drought, A. B., and Kory, R. C. (1964). Walking patterns of normal men. *J. Bone Joint Surg. Am.* 46, 335–360. doi: 10.2106/00004623-196446020-00009

Nemcova, A., Jordanova, I., Varecka, M., Smisek, R., Marsanova, L., Smital, L., et al. (2020). Monitoring of heart rate, blood oxygen saturation, and blood pressure using a smartphone. *Biomed. Signal Process. Control* 59:101928. doi: 10.1016/j.bspc.2020.101928

Rajasekaran, V., López-Larraz, E., Trincado-Alonso, F., Aranda, J., Montesano, L., Del-Ama, A. J., et al. (2018). Volition-adaptive control for gait training using wearable exoskeleton: preliminary tests with incomplete spinal cord injury individuals. *J. Neuroeng. Rehabil.* 15, 1–15. doi: 10.1186/s12984-017-0345-8

Rasmussen, C. E., and Williams, C. (2006). *Gaussian Processes for Machine Learning*. Cambridge, MA: The MIT Press.

Reddy, M. K., and Rani, S. (2016). Statistical image compression using fast fourier coefficients. *Int. J. Comput. Appl.* 155. doi: 10.5120/ijca2016912282

Riener, R., Lünenburger, L., Maier, I. C., Colombo, G., and Dietz, V. (2010). Locomotor training in subjects with sensori-motor deficits: an overview of the robotic gait orthosis lokomat. *J. Healthc. Eng.* 1, 197–216. doi: 10.1260/2040-2295.1.2.197

Santos, V., Moreira, R., and Silva, F. (2012). Mechatronic design of a new humanoid robot with hybrid parallel actuation. *Int. J. Adv. Rob. Syst.* 9, 119. doi: 10.5772/51535

Stauffer, Y., Allemand, Y., Bouri, M., Fournier, J., Clavel, R., Métrailler, P., et al. (2008). The walktrainer–a new generation of walking reeducation device combining orthoses and muscle stimulation. *IEEE Trans. Neural Syst. Rehabil. Eng.* 17, 38–45. doi: 10.1109/TNSRE.2008.2008288

Trivino, G., Alvarez-Alvarez, A., and Bailador, G. (2010). Application of the computational theory of perceptions to human gait pattern recognition. *Pattern Recognit.* 43, 2572–2581. doi: 10.1016/j.patcog.2010.01.017

Tsukahara, A., Hasegawa, Y., Eguchi, K., and Sankai, Y. (2014). Restoration of gait for spinal cord injury patients using hal with intention estimator for preferable swing speed. *IEEE Trans. Neural Syst. Rehabil. Eng.* 23, 308–318. doi: 10.1109/TNSRE.2014.2364618

Tsumoto, S., and Hirano, S. (2014). "Formal analysis of leave-one-out methods based on decremental sampling scheme," in *2014 IEEE/WIC/ACM International Joint Conferences on Web Intelligence (WI) and Intelligent Agent Technologies (IAT)*, Vol. 2 (San Diego, CA: IEEE), 371–378.

Vallery, H., Van Asseldonk, E. H., Buss, M., and Van Der Kooij, H. (2008). Reference trajectory generation for rehabilitation robots: complementary limb motion estimation. *IEEE Trans. Neural Syst. Rehabil. Eng.* 17, 23–30. doi: 10.1109/TNSRE.2008.2008278

Wang, L., Tan, T., Ning, H., and Hu, W. (2003). Silhouette analysis-based gait recognition for human identification. *IEEE Trans. Pattern Anal. Mach. Intell.* 25, 1505–1518. doi: 10.1109/TPAMI.2003.1251144

Winter, D. A. (2009). *Biomechanics and Motor Control of Human Movement*. Hoboken, NJ: John Wiley & Sons.

Wong, T.-T. (2015). Performance evaluation of classification algorithms by k-fold and leave-one-out cross validation. *Pattern Recognit.* 48, 2839–2846. doi: 10.1016/j.patcog.2015.03.009

Yun, Y., Kim, H.-C., Shin, S. Y., Lee, J., Deshpande, A. D., and Kim, C. (2014). Statistical method for prediction of gait kinematics with gaussian process regression. *J. Biomech.* 47, 186–192. doi: 10.1016/j.jbiomech.2013.09.032

Zhang, Y., and Ma, Y. (2019). Application of supervised machine learning algorithms in the classification of sagittal gait patterns of cerebral palsy children with spastic diplegia. *Comput. Biol. Med.* 106, 33–39. doi: 10.1016/j.compbiomed.2019.01.009

Zhang, Z., Dong, Y., Ni, F., Jin, M., and Liu, H. (2015). A method for measurement of absolute angular position and application in a novel electromagnetic encoder system. *J. Sens.* 2015:503852. doi: 10.1155/2015/503852